Journal of Materials Processing Technology 239 (2017) 315–325

Contents lists available at ScienceDirect

Journal of Materials Processing Technology

journal homepage: www.elsevier.com/locate/jmatprotec

Dynamic recrystallization behaviour of spheroidal graphite iron. Application to cutting operations

K. Le Mercier[a,c,*], M. Watremez[a,c], E.S. Puchi-Cabrera[a,c], L. Dubar[a,c], J.D. Guérin[a,c], L. Fouilland-Paillé[b,c]

[a] UVHC, LAMIH UMR CNRS 8201, F-59313 Valenciennes, France
[b] Arts et Metiers ParisTech, MSMP EA7350, F-51006 Châlons en Champagne, France
[c] Institut Carnot Arts, F-75013 Paris, France

ARTICLE INFO

Article history:
Received 3 February 2016
Received in revised form 29 August 2016
Accepted 30 August 2016
Available online 2 September 2016

Keywords:
SG iron
Hot cutting
Dynamic recrystallization
Finite element modelling

ABSTRACT

To increase the competitiveness of manufacturing processes, numerical approaches are unavoidable. Nevertheless, a precise knowledge of the thermo-mechanical behaviour of the materials is necessary to simulate accurately these processes. Previous experimental studies have provided a limited information concerning dynamic recrystallization of spheroidal graphite iron under hot cutting operations. The purpose of this paper is to develop a constitutive model able to describe accurately the occurrence of this phenomenon. Compression tests are carried out using a Gleeble 3500 thermo-mechanical simulator to determine the hot deformation behaviour of spheroidal graphite iron at high strains. Once the activation range of the dynamic recrystallization process is assessed, a constitutive model taking into account this phenomenon is developed and implemented in the Abaqus/Explicit software. Finally, a specific cutting test and its finite element model are introduced. The ability of the numerical model to predict the occurrence of dynamic recrystallization is then compared to experimental observations.

1. Introduction

Over the past few years, austempered ductile iron emerged for its application in several fields such as automotive and railway industries. This specific spheroidal graphite iron provides an efficient compromise between specific mechanical strength, fracture toughness and resistance to abrasive wear. Therefore, this material is intended to substitute forged steels for the weight reduction of numerous manufactured components (Kovacs, 1987). To reach these enhanced mechanical properties, austempered ductile iron is obtained by a specific thermo-mechanical treatment (Fig. 1). This consists in an austenitization of the cast iron in the temperature range 1123–1223 K followed by quenching to an austempering temperature of 523–623 K causing the transformation of the austenite phase into ausferrite. A combined casting and forging process prior to this specific quenching is often performed to reduce manufacturing costs (Meena and El Mansori, 2012). Also, with the aim of increasing the competitiveness, the removal of risers and feeder head is then performed at about 1273 K just after the casting operation. However, this stage can give rise to severe surface degradations under the cut surface, compromising the process viability.

A recent experimental investigation, performed by Fouilland and El Mansori (2013), allowed a better understanding of the mechanisms involved during the hot cutting of cast specimens. During this operation, spheroidal graphite iron is stabilized in the austenite phase. The main softening process of austenite is dynamic recrystallization (DRX) due to its low stacking fault energy (Mirzadeh and Najafizadeh, 2010). Indeed, given the crystalline structure of austenite (fcc), cross-slip of dislocations is restricted and work hardening (WH) is only slightly moderated by dynamic recovery (DRV). The kinetic of DRV is too slow and the DRX process can then occur. The study of Fouilland and El Mansori (2013) revealed that the appearance of surface degradations is governed by a brittle–ductile transition, depending on the occurrence of DRX. When this softening process takes place a ductile behaviour leading to a precise cut is observed. Otherwise, a brittle behaviour arises promoting deep crack propagation under the cut surface.

The plastic flow stress evolution of a material which undergoes DRX is shown schematically in Fig. 2. At stresses less than the critical stress for the onset of DRX (σ_c), the material undergoes both WH and DRV. However, once σ_c is exceeded DRX will become operative and the three processes will occur simultaneously. As the strain

* Corresponding author at: UVHC, LAMIH UMR CNRS 8201, F-59313 Valenciennes, France.
E-mail address: kevin.lemercier@univ-valenciennes.fr (K. Le Mercier).

http://dx.doi.org/10.1016/j.jmatprotec.2016.08.036
0924-0136/

Nomenclature

Abbreviations

DIC	digital image correlation
DRV	dynamic recovery
DRX	dynamic recrystallization
JMAK	Johnson–Mehl–Avrami–Kolmogorov model
SGI	spheroidal graphite iron
STG	Sellars–Tegard–Garofalo model
WH	work hardening

Arabic symbols

A	material parameter
B_s, B_{ss}, B_y	material parameters in the STG model, s^{-1}
D	material parameter, s
m_s, m_{ss}, m_y	material parameters in the STG model
n_{Av}	Avrami exponent
Q	apparent activation energy for hot-working, kJ mol^{-1}
q	material parameter
Q_{DRX}	apparent activation energy for dynamic recrystallization, kJ mol^{-1}
R	universal gas constant, J mol^{-1} K^{-1}
T	absolute temperature, K
t	time during which DRX occurs, s
$t_{0.5}$	time for 50 percent recrystallization, s
X_v	volume fraction recrystallized
Z	Zener–Hollomon parameter, s^{-1}

Greek symbols

δ_s, δ_{ss}, δ_y	material parameters in the STG model, MPa
ε	total effective strain
$\dot{\varepsilon}$	effective strain rate, s^{-1}
ε_c	critical strain for the onset of DRX
ε_r	relaxation strain
θ_0	work hardening rate of the material
$\mu(T)$	temperature-dependent shear modulus, MPa
Σ	flow stress defined in the user subroutine, MPa
σ	flow stress after the onset of DRX, MPa
σ_c	critical stress for the onset of DRX, MPa
σ_ε	flow stress corresponding to the WH and DRV curve, MPa
σ_{eq}	equivalent von Mises stress, MPa
σ_p	peak stress, MPa
$\sigma_{sat}(T, \dot{\varepsilon})$	hypothetical saturation stress, MPa
$\sigma_{ss}(T, \dot{\varepsilon})$	steady-state flow stress, MPa
$\sigma_y(T, \dot{\varepsilon})$	yield stress, MPa

applied to the material increases, the volume fraction recrystallized dynamically (X_v) will also increase and supersede the effect of WH and DRV. As a consequence, a work softening transient will occur, leading to the presence of a peak stress (σ_p) on the flow stress curve. As the strain applied to the material continuous to increase, the balance among WH, DRV and DRX will lead to the achievement of a steady-state stress (σ_{ss}), whose magnitude is equal to σ_c.

In numerical cutting models, the Johnson and Cook (1983) constitutive formulation is generally implemented because of its simplicity and numerical robustness (Limido et al., 2007). However, this empirical law describes the flow stress as a function of the total strain applied to the material, which is not a valid state parameter, by means of a simple parametric power-law relationship. Such a description would be incompatible with the evolution of flow stress mentioned above. Therefore, the present paper deals with the development of a specific constitutive model which not only allows the DRX process to be considered, but also that expresses the flow stress in terms of valid state parameters. Thus, the first challenge is to determine the activation range in which DRX occurs, by means of hot compression tests. Then, the selected model is implemented in the finite element analysis of a specific cutting operation. Finally, the prediction of the numerical model concerning the occurrence of DRX is discussed in relation to the experimental observations.

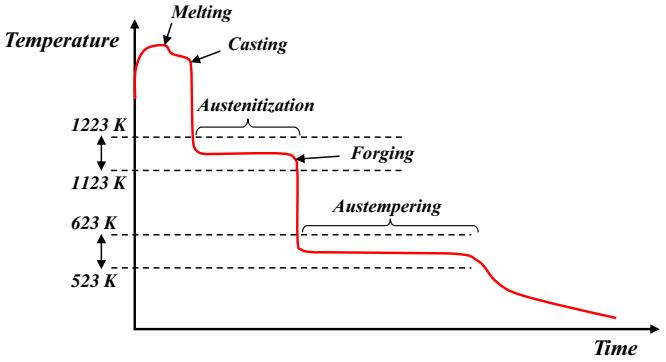

Fig. 1. Heat treatment example for austempered ductile iron.

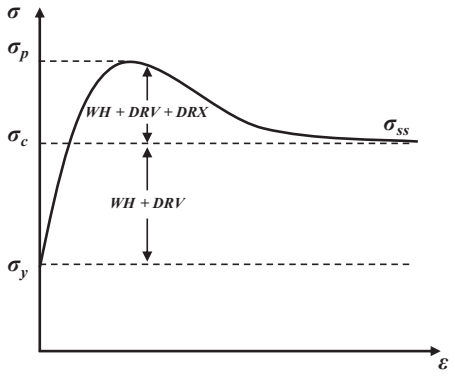

Fig. 2. Typical dynamic recrystallization hardening curve.

2. Experimental techniques

2.1. Material

The material employed for the present study is an ASTM A536 100-70-03 iron similar to that employed by Fouilland and El Mansori (2013). This spheroidal graphite iron (SGI) exhibits a pearlitic matrix at room temperature and a small amount of ferrite surrounding the graphite nodules, called bullseye ferrite (Fig. 3). Its chemical composition is given in Table 1.

2.2. Mechanical characterization

The experiments were performed on a Gleeble 3500 thermo-mechanical testing machine. Compression specimens of 10 mm in diameter and 12 mm in length were tested under constant deformation conditions in a vacuum chamber. The samples were heated at 5 K s^{-1} to the testing temperature and then held for 1 min at the test temperature. A K-thermocouple was welded at the half height of the specimen to ensure the temperature measurement. The tests were conducted at mean effective strain rates of 0.5, 1 and 5 s^{-1}, at nominal temperatures of 1073, 1173 and 1273 K. At the end of the tests, the specimens were air cooled. At least two tests were conducted for each deformation condition.